International Journal of Bifurcation and Chaos, Vol. 25, No. 7 (2015) 1540002 (17 pages)

DOI: 10.1142/S0218127415400027

Synchrony in Metapopulations with Sporadic Dispersal

Russell Jeter and Igor Belykh*
Department of Mathematics and Statistics and Neuroscience Institute, Georgia State University, 30 Pryor Street, Atlanta, GA 30303, USA
**ibelykh@gsu.edu*

Received April 4, 2015

We study synchronization in ecological networks under the realistic assumption that the coupling among the patches is sporadic/stochastic and due to rare and short-term meteorological conditions. Each patch is described by a tritrophic food chain model, representing the producer, consumer, and predator. If all three species can migrate, we rigorously prove that the network can synchronize as long as the migration occurs frequently, i.e. fast compared to the period of the ecological cycle, even though the network is disconnected most of the time. In the case where only the top trophic level (i.e. the predator) can migrate, we reveal an unexpected range of intermediate switching frequencies where synchronization becomes stable in a network which switches between two nonsynchronous dynamics. As spatial synchrony increases the danger of extinction, this counterintuitive effect of synchrony emerging from slower switching dispersal can be destructive for overall metapopulation persistence, presumably expected from switching between two dynamics which are unfavorable to extinction.

Keywords: Tritrophic models; stochastic dispersal; synchronization.

1. Introduction

Synchronization of the growth cycles in ecological networks of multispecies populations, called metapopulations, across a geographic region has been widely documented and studied (see, for example, [Ranta *et al.*, 1995; Earn *et al.*, 2000; Colombo *et al.*, 2008] and the references therein). Multiple examples of population synchronization include moths and butterflies [Hanski & Woiwod, 1993; Johnson *et al.*, 2005], crabs [Higgins *et al.*, 1997], fish [Ranta *et al.*, 1995], birds [Cattadori *et al.*, 1999], hares [Ranta *et al.*, 1995], lynx [Elton & Nicholson, 1942] and sheep [Grenfell *et al.*, 1998].

The first example of population synchrony was given in the study of fur returns of Canadian lynx to the Hudson Bay Company [Elton, 1924]. The cause for spatial synchrony is believed to be a combination of correlated atmospheric conditions (the Moran effect) [Ranta *et al.*, 1997; Cazelles & Boudjema, 2001; Colombo *et al.*, 2008; He *et al.*, 2010] and the presence of migration between population patches. Synchronization of Canadian lynx was initially attributed to the Moran effect; however, several studies have indicated that sufficiently strong dispersal in networks of tritrophic food chain models, related to the Canadian boreal forest, can induce synchrony without common atmospheric conditions (see for example, [Blasius *et al.*, 1999; Belykh *et al.*, 2009]). These studies supported by the DNA analysis [Schwartz *et al.*, 2002], revealing high dispersal of Canadian lynx over large distance between the East and West Coasts, suggest that dispersal plays a key role in the spatial synchronization of the Canadian lynx. Moreover, there are numerous

*Author for correspondence

factors which can influence both the frequency and rate at which species migrate, and subsequently inhibit or promote spatial synchrony. It is generally accepted that the Moran effect is typically responsible for synchrony on the continental scale, whereas migration facilitates local, metapopulation synchrony.

In most theoretical studies, the migration is assumed to be a continuous process with net migration flow proportional (through a constant dispersal coefficient) to the unbalance of population densities. Under this assumption, the metapopulation model is an n-patch network of linearly coupled food-chain models with a static graph. The static interaction is typically assumed to be of diffusive nature (on an arbitrary coupling graph) and defined by a zero-row sum connection matrix (see, for example, [Belykh *et al.*, 2009]). There has also been a fair amount of work focused on density dependent migration models (for example, a model where predator migration is dependent on the prey density in a given patch [Huang & Diekmann, 2001]). However, a more realistic assumption could be that the dispersal among the patches is not constant, but of intermittent nature. More precisely, migration episodes are due to rare and short-term particular meteorological conditions such as high winds or strong water currents, but occur relatively frequently during the period of the ecological cycle. The prominent example of an ecological network with random, "blinking" interactions is a chain of lakes connected via narrow, shallow channels where the migration of algae and zooplankton is due to weak, random water currents. These sporadic algae-zooplankton interactions among the lakes have been shown to trigger synchronous algae outbreaks and crashes, resulting in synchronous clear water episodes in Lake Lugano, Switzerland [Ravera, 1977; Rinaldi, 2009]. Synchronization of insect-pest outbreaks in forests, connected by high, but sporadic winds has also been largely debated (see [Rinaldi, 2012] and the references therein).

When considering migration within a metapopulation, it is natural to think of the metapopulation as a network of patches that is sporadically connected through migration routes by which species can travel from a patch to a nearby patch, such as, e.g. insects dispersing using favorable wind conditions. This means that to model the inherent stochasticity in the migration, we can turn the links between nodes in the network "on" and "off" randomly. This requires that both the time scale of the metapopulation and the stochastic process be considered in modeling (see [Levin, 1992; Chave, 2013; Cantrell *et al.*, 2009] for the discussion on the problem of pattern and scale in Ecology). While stochastic dispersal and its role in population persistence have received a great deal of attention (see [Williams & Hastings, 2013]), the patches are typically assumed to have simple dynamics and often described by simple discrete-time models.

In this paper, we aim at the hardest case where individual patches can have chaotic dynamics which are described by the tritrophic Rosenzweig–MacArthur model [Rosenzweig & MacArthur, 1963]; in addition, one of the intrinsic parameters and the on–off dispersal between the patches are stochastic, with their own time scales, ranging from fast to slow. We put the general blinking network model [Belykh *et al.*, 2005a] with fast on–off stochastic connections into the ecological context and use the rigorous theory [Hasler *et al.*, 2013a, 2013b; Belykh *et al.*, 2013] on probabilistic convergence to derive upper bounds on the switching frequency of on–off dispersal to achieve approximate synchronization in the stochastic metapopulation network in the fast switching limit. More precisely, we show that if the migration of all three species is allowed, the stochastic ecological network converges to approximate synchrony globally and almost surely as long as the switching is fast and the dispersal strength is sufficiently strong to guarantee synchronization in the averaged network, obtained by replacing the stochastic variables with their means. Going beyond fast switching, we report a counterintuitive effect when non-fast switching makes synchronization stable even though it is unstable in the averaged/fast switching network. In this case, the network, switching between two non-synchronous states, each of which supports population persistence, can promote spatial synchrony and therefore increase the risk of extinction. We show that the effect is maximized when the probability of switching p is close to $1/2$, suggesting a stabilizing effect of the most probable reswitching.

The layout of this paper is as follows. First, in Sec. 2, we introduce the stochastic model and discuss its synchronization properties. Then, in Sec. 3, we consider the fast switching case and give the reader background on the blinking systems theory [Hasler *et al.*, 2013a, 2013b; Belykh *et al.*, 2013]. We formally state the main theorem, in which we derive

explicit analytical upper bounds for the switching frequency for migration that guarantees synchrony. While we would ideally like to lead the reader through all of the ins and outs of the proof, we recognize some of the details are too technical (and spatially cumbersome) to include in the main text. For this reason, the majority of the proof can be found in the Appendix. In Sec. 4, we consider the case in which the switching is not fast (relative to the time scale of the ecological system), but not too slow. We find somewhat striking results for this intermediate switching case, for which a rigorous theory has not yet been established. Finally, in Sec. 5, a brief discussion of the obtained results is given.

2. The Model and Problem Statement

2.1. *Individual patch model*

We use the tritrophic extension of the Rosenzweig–MacArthur prey–predator model [Rosenzweig & MacArthur, 1963] as the individual patch in the metapopulation stochastic network. The individual model reads

$$\begin{cases} \dot{x} = rx\left(1 - \dfrac{x}{K}\right) - \dfrac{a_1 xy}{1 + a_1 b_1 x} \\ \dot{y} = \dfrac{a_1 xy}{1 + a_1 b_1 x} - m_1 y - \dfrac{a_2 yz}{1 + a_2 b_2 y} \\ \dot{z} = \dfrac{a_2 yz}{1 + a_2 b_2 y} - m_2 z, \end{cases} \tag{1}$$

where x, y, and z are the producer, consumer, and predator population densities, respectively, r and K are the growth rate and carrying capacity of the producer, while a_1 and a_2 are conversion rates (a_1 from producer to consumer and a_2 from consumer to predator), with their respective saturation constants being b_1 and b_2. Lastly, m_1 and m_2 are the mortality rates of the consumer and predator, respectively. The model (1) can exhibit periodic and chaotic behaviors, including Shilnikov-type chaos [Deng & Hines, 2001; Kuznetsov *et al.*, 2001]. Hereafter, the mortality rate of the predator population m_2 is assumed to be lower than that of the consumer m_1 as the predators typically have a longer life span than the consumer (e.g. fish versus zooplankton in the algae-zooplankton-fish food chain). This assumption together with a high carrying capacity of the producer, K, typically leads to chaotic dynamics in the patch. Unless specified otherwise, the values of parameters $r = 1.15$, $K = 1.07$, $a_1 = 5$, $b_1 = 0.6$, $m_1 = 0.4$, $a_2 = 0.1$, $b_2 = 20$, $m_2 = 0.0037$ are chosen and fixed to place the individual model in a chaotic regime (see Fig. 1).

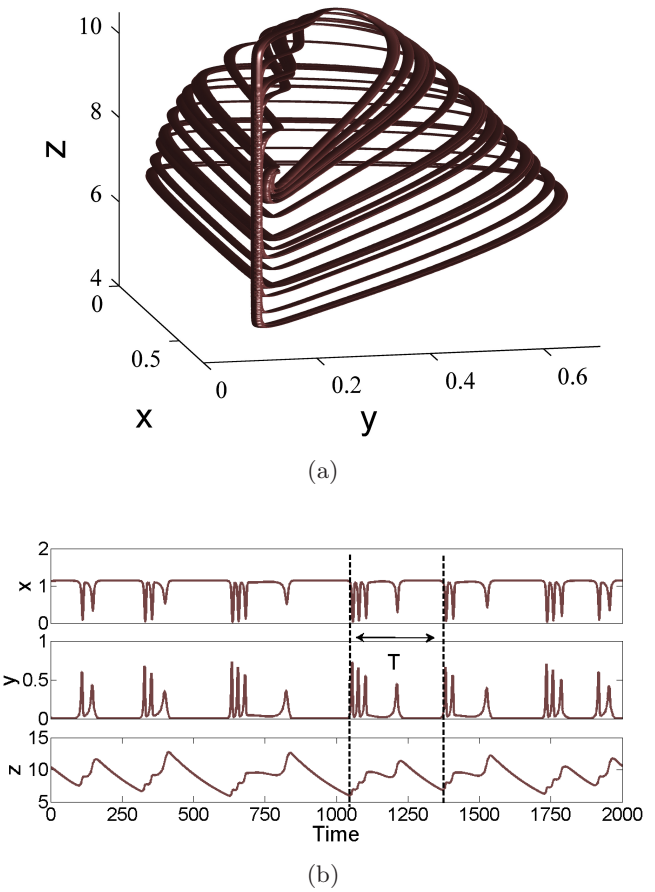

Fig. 1. (a) The chaotic attractor of the uncoupled patch model (1). The attractor resembles an upside down tea cup shape; hence inspiring the artistic presentation of its trajectories as dipped in chocolate. (b) The corresponding time series. The top, middle, and bottom graphs give the time series for x, y, and z, respectively. The population size is given in a dimensionless unit. The dashed lines indicate the beginning and end of a population cycle, the characteristic period (T) of the metapopulation, which is approximately $T = 200$ units of time.

2.2. *The stochastic network*

Introduced in [Belykh *et al.*, 2005a], the general "blinking" network [Hasler *et al.*, 2013a, 2013b] fits well with the peculiar nature of random, sporadic interaction between metapopulations and can be used as the main tool in the study of synchronization in ecological models with realistic sporadic interactions. We consider a network composed of n tritrophic Rosenzweig–MacArthur prey–predator

models (1), interconnected pairwise via stochastic dispersal:

$$\begin{cases} \dot{x}_i = rx_i\left(1-\dfrac{x_i}{K}\right) - \dfrac{[a_1+\Delta a\xi_i(t)]x_iy_i}{1+a_1b_1x_i} \\ \qquad\qquad + \varepsilon_x\displaystyle\sum_{j=1}^{n} s_{ij}(t)(x_j-x_i) \\ \dot{y}_i = \dfrac{[a_1+\Delta a\xi_i(t)]x_iy_i}{1+a_1b_1x_i} - m_1y_i \\ \qquad\qquad - \dfrac{a_2y_iz_i}{1+a_2b_2y_i} + \varepsilon_y\displaystyle\sum_{j=1}^{n} s_{ij}(t)(y_j-y_i) \\ \dot{z}_i = \dfrac{a_2y_iz_i}{1+a_2b_2y_i} - m_2z_i \\ \qquad\qquad + \varepsilon_z\displaystyle\sum_{j=1}^{n} s_{ij}(t)(z_j-z_i), \quad i=1,\ldots,n, \end{cases} \tag{2}$$

where ε_x, ε_y, and ε_z are the coupling strengths (strengths of dispersal of the producer, consumer, and predator populations, respectively). Stochastic variables $s_{ij}(t)$ form the time-varying connectivity (Laplacian) matrix $C(t)$. Following [Belykh *et al.*, 2005a; Hasler *et al.*, 2013a, 2013b], we define the stochastic variables s_{ij} as follows: we divide the time axis into intervals of length τ; we then assume $s_{ij}(t)$ to be binary signals that take the value 1 with probability p and the value 0 with probability $1-p$ in each time interval. The existence of an edge from vertex i to vertex j is determined randomly and independently of other edges with probability $p_{ij} \in [0,1]$. Expressed in words, every migration link in the metapopulation network turns on and off, according to a similar probability law, and the migration between any two patches opens and closes in different time intervals independently. All possible migration links $s_{ij} = s_{ji}$ are allowed to turn on and off so that the metapopulation network $C(t)$ remains constant during each time interval $[k\tau,(k+1)\tau)$ between the reswitching and represents an Erdös–Rényi graph of n vertices (see Fig. 2). Such stochastically blinking networks represent an example of evolving dynamical networks whose synchronization and control [Porfiri *et al.*, 2006; Lü & Chen, 2005; Frasca *et al.*, 2008; Sorrentino & Ott, 2008; So *et al.*, 2008; De Lellis *et al.*, 2010] are highly active research directions, with multiple applications in technological, animal,

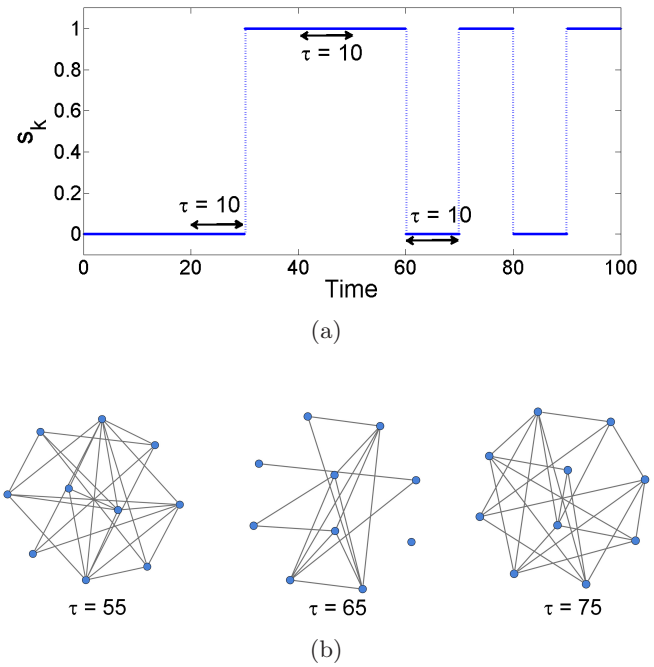

Fig. 2. (a) Example of the stochastic process with $p = 0.5$ and $\tau = 10$. The time axis is divided into intervals of length τ; for each interval, $s_k = 1$ with probability p and $s_k = 0$ with probability $1-p$. (b) Three different instances of the same stochastically switching network. Note one disconnected node in the network at $\tau = 65$, making network synchronization impossible during this lapse of time.

and neuronal networks (see a review paper [Belykh *et al.*, 2014] and the references therein).

The stochastically blinking sporadic interactions $s_{ij}(t)$ in the network (2) describe the stochastic opening of migration corridors when conditions are favorable (such as, e.g. heavy rains allowing fish to migrate to another lake through streams that are normally too shallow to traverse). It is also reasonable to assume that the intrinsic parameters of the individual patch model (1) can also be stochastic functions, similar to $s_{ij}(t)$. For example, when producer–consumer interaction rate a_1 switches between two different values based on some stochastic process; for instance, when the weather is especially fierce, a rabbit may not leave his burrow to eat grass. To account for this intrinsic stochasticity in patch i, we have replaced the traditional parameter a_1 [cf. (1)] with $[a_1 + \Delta a\xi_i(t)]$, where $\xi_i(t)$ is a stochastic variable. For simplicity, we assume that $\xi_i(t)$ is governed by the same stochastic process (but by a different stochastic sequence) and can switch on and off at the same times as $s_{ij}(t)$. For example, strong winds, allowing the migration of insects between nearby patches, can also prevent

the insects, already present in the patches, from food searching, thereby affecting parameter a_1.

This intrinsic stochasticity parameter makes the patches, comprising the network (2), nonidentical such that complete synchronization between the patches is no longer possible. However, approximate synchronization with fluctuating synchronization errors can be observed in this metapopulation network with stochastic connections and intrinsic parameters. Thus, we have knowingly decided to handle approximate synchronization in the mismatched network that better represents realistic ecological systems with no perfect symmetries. In the next section, we will derive sufficient stability conditions of approximate synchronization in the stochastic network. The generalization of all the results of this paper to networks of identical patches is straightforward.

3. Fast Switching

3.1. *Switching versus averaged networks*

If dispersal switching is fast compared to the ecological cycle of the individual patch, one can expect the behavior of the stochastic network (2) to be close to that of the averaged network, obtained by replacing the stochastic variables $s_{ij}(t)$ and $\xi_i(t)$ by their expected value, the switching probability p. Hence, the averaged network is an all-to-all coupled static network with weaker connections:

$$\begin{aligned}
\dot{x}_i &= rx_i\left(1-\frac{x_i}{K}\right) - \frac{[a_1+\Delta a\cdot p]x_iy_i}{1+a_1b_1x_i} \\
&\quad + \varepsilon_x p\sum_{j=1}^{n}(x_j-x_i) \\
\dot{y}_i &= \frac{[a_1+\Delta a\cdot p]x_iy_i}{1+a_1b_1x_i} - m_1y_i \\
&\quad - \frac{a_2y_iz_i}{1+a_2b_2y_i} + \varepsilon_y p\sum_{j=1}^{n}(y_j-y_i) \\
\dot{z}_i &= \frac{a_2y_iz_i}{1+a_2b_2y_i} - m_2z_i + \varepsilon_z p\sum_{j=1}^{n}(z_j-z_i).
\end{aligned} \tag{3}$$

The fact that the fast switching network has the same dynamics as the averaged network seems apparent; however, there are exceptions and a rigorous proof is needed to show what parameters are responsible for the occurrence of the exceptions. A complete rigorous theory for the behavior of stochastically switching networks that switch rapidly was developed in [Hasler *et al.*, 2013a, 2013b]. The difference between the dynamics of switching and averaged networks is especially pronounced when the averaged network is multistable such that the trajectory of the switching network may converge to the targeted attractor with high probability or may escape towards another attractor [Hasler & Belykh, 2005]. This general theory [Hasler *et al.*, 2013a, 2013b] derives explicit bounds for these probabilities and relates them to the switching frequency, the precision, and the length of the time interval (see its application to a multistable switching oscillator in [Belykh *et al.*, 2013]).

In the following, we apply this theory to synchronization in the ecological network (2) and derive bounds on the switching frequency that guarantees stable synchronization. Note that synchronization in the static averaged network (3) of identical patches is defined by the invariant hyperplane $M=\{x_1=x_2=\cdots=x_n, y_1=y_2=\cdots=y_n, z_1=z_2=\cdots=z_n\}$. At the same time, this hyperplane is no longer invariant under the dynamics of the switching network (2) with stochastically mismatched parameters $[1+\Delta a\xi_i(t)]a_1$. Therefore, only approximate synchronization, when trajectories of the switching network approach and stay in a δ-neighborhood of the "ghost" synchronization solution is possible. We shall show that under the condition that the averaged network exhibits globally stable synchronization, the switching network reaches approximate synchronization, provided that the switching period is sufficiently small. While expected, this effect is not obvious as the switching network is disconnected most of the time, yet is able to synchronize.

3.2. *Synchronization in the averaged network*

Before proceeding with the study of the stochastic network, we should first understand the synchronization properties of the averaged network. Following [Belykh *et al.*, 2009], we explore several scenarios of possible migration schemes between ecological patches when all three trophic levels (x, y, z-coupling) or only one trophic level can migrate. Figure 3 presents the Master Stability function [Pecora & Carroll, 1998] for synchronization in the averaged network. As Fig. 3

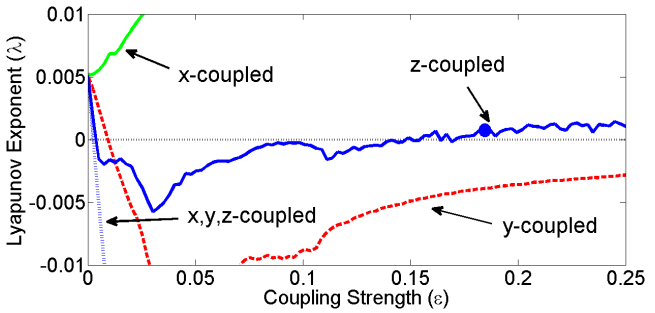

Fig. 3. The largest transversal Lyapunov exponent (λ) versus coupling strength ε for the two-patch x-coupled (green curve), y-coupled (red, dashed curve), z-coupled (blue curve) and x, y, z-coupled (blue, dotted curve) averaged network (3). $\lambda < 0$ corresponds to stable synchronization. While the x, y, z-coupled system is stable for all $\varepsilon > \varepsilon^*_{xyz} = 0.002$ (not shown), the z-coupled system has a window of stability, outside of which the patches exhibit asynchronous behavior. The solid circle (•) indicates the value of $\varepsilon = 0.175$ used in the calculations for the non-fast switching case of Fig. 5.

suggests, the x, y, z-coupling when three species can migrate is the most effective mechanism for promoting spatial synchrony. Notice that the x, y, z-coupling has the lowest synchronization threshold $\varepsilon_x = \varepsilon_y = \varepsilon_z = \varepsilon = \varepsilon^*_{xyz}$ among the four migration schemes; and the largest stability zone, expanding to the right from $\varepsilon^*_{xyz} = 0.002$ up to infinite coupling strengths. If only one species can migrate, the dispersal of the consumer (i.e. the intermediate trophic level) is the most effective in establishing spatial synchrony. Notice that the dispersal of only the producer (x-coupling) never induces synchrony, whereas the dispersal of the predator (z-coupling) yields a bounded stability well such that increasing the dispersal strength ε_z eventually destabilizes the synchronization solution. The latter property of the z-coupled migration scheme will be used later in the paper to discuss synchronization in the non-fast switching case.

We choose the most effective migration scheme of x, y, z-coupling with $\varepsilon_x = \varepsilon_y = \varepsilon_z = \varepsilon$ to study synchronization in the averaged network (3) and approximate synchronization in the stochastic network (2). We first formulate conditions on the coupling strength sufficient for global stability of the synchronization hyperplane M.

Theorem 1. *Synchronization in the averaged x, y, z-coupled network (3) of n patches with coupling strength $p\varepsilon_x = p\varepsilon_y = p\varepsilon_z = p\varepsilon$ and the averaged intrinsic parameter $a_1^* = [1 + \Delta a \cdot p]a_1$ is globally asymptotically stable if coupling ε exceeds the critical value*

$$\varepsilon^* = \frac{1}{p}\max\{\varepsilon_1, \varepsilon_2, \varepsilon_3, \varepsilon_4, \varepsilon_5\},$$

$$\text{such that } p\varepsilon_1 > \frac{r}{n}; \quad p\varepsilon_2 > \frac{1}{n}\left[\frac{1}{b_1} - m_1\right];$$

$$p\varepsilon_3 > \frac{1}{n}\left[\frac{1}{b_2} - m_2\right]$$

$$(n\varepsilon_4 - r)\left(n\varepsilon_4 + m_1 - \frac{1}{b_1}\right) > \frac{1}{2b_1^2};$$

$$\left(n\varepsilon_5 + m_1 - \frac{1}{b_1}\right)\left(n\varepsilon_5 + m_2 - \frac{1}{b_2}\right) > \frac{1}{2b_2^2}. \tag{4}$$

Proof. The proof directly follows from the one given in [Belykh *et al.*, 2009] for the two-patch static network (3) (see Appendix in [Belykh *et al.*, 2009]) where the coupling ε is replaced with $p\varepsilon$ and the network is extended to the all-to-all configuration with n patches. ■

This bound can be generalized to more complex averaged network topologies, corresponding to networks with given switching connections that are not all-to-all, by using the Connection Graph method [Belykh *et al.*, 2005b]. The proof also involves the construction of the absorbing domain, giving a lower bound for the trajectories of the averaged network. As this bound will be used in the conditions of the main theorem (Theorem 2), related to fast switching, we present its derivation in the following subsection.

3.3. *Absorbing domain*

To get the lower bound for trajectories of the averaged network (3) with $\varepsilon_x = \varepsilon_y = \varepsilon_z = \varepsilon$, we notice upon examining (3) that the trajectories may not leave the region $A^+ = \{x_i > 0, y_i > 0, z_i > 0\}$ for initial conditions $x_i, y_i, z_i \geq 0$ such that the system is restricted to the positive orthant of R^{3n}. Next, we must show that the system (3) is bounded in that orthant as well. To do this, we will introduce the following function:

$$V = \sum_{i=1}^{n}(x_i + y_i + z_i - \varphi), \tag{5}$$

where φ is a constant to be determined. We need to find the constant φ that makes V a Lyapunov-type function such the vector field of (3) on levels of V is oriented towards the origin.

We take the derivative of V with respect to system (3) and get

$$\dot{V} = \sum_{i=1}^{n} (\dot{x}_i + \dot{y}_i + \dot{z}_i)$$

$$= \sum_{i=1}^{n} \left(r x_i \left(1 - \frac{x_i}{K}\right) - m_1 y_i - m_2 z_i \right), \quad (6)$$

where the terms $\pm\frac{[a_1+\Delta ap]x_i y_i}{1+a_1 b_1 x_i}$ and $\pm\frac{a_2 y_i z_i}{1+a_2 b_2 y_i}$ and the coupling terms have canceled out.

Using the assumption that $m_1 > m_2$ (which is a natural assumption in ecological models), we can bound the RHS of (6) by replacing the term $m_1 y_i$ with $m_2 y_i$. This yields

$$\dot{V} < \sum_{i=1}^{n} \left(r x_i \left(1 - \frac{x_i}{K}\right) - m_2 (y_i + z_i) \right)$$

$$< \sum_{i=1}^{n} \left(r x_i - \frac{r x_i^2}{K} - m_2 (\varphi - x_i) \right)_{V=0}, \quad (7)$$

where we have replaced the term $m_2(y_i + z_i)$ with its minimum value $m_2(\varphi - x_i)$, reached at $V = \sum_{i=1}^{n} (x_i + y_i + z_i - \varphi) = 0$ and, hence, $y_i + z_i = \varphi - x_i$. Therefore,

$$\dot{V} < \sum_{i=1}^{n} \left(r x_i \left(1 - \frac{x_i}{K}\right) - m_2 (\varphi - x_i) \right) \quad (8)$$

which implies that $\dot{V} < 0$ if $\varphi > \psi$, where

$$\psi = \frac{K}{4 r m_2} (r + m_2)^2. \quad (9)$$

This means that the region of the positive orthant bounded by V_ψ is an absorbing domain such that $0 \le x_i, y_i, z_i \le \psi$.

3.4. *Stochastic networks: Rigorous bounds*

The general theory of fast switching (blinking) networks [Hasler *et al.*, 2013a, 2013b] involves finding upper bounds on the first and second time derivatives of the Lyapunov function W, calculated along solutions of the averaged and switching systems. This Lyapunov function guarantees the convergence to the desired attractor in the averaged system and should be proven to provide probabilistic convergence towards the corresponding attractor (or its ghost) in the switching system.

In our context, this is the Lyapunov function

$$W = \sum_{i=1}^{n} \sum_{j>i}^{n} \frac{1}{2} (X_{ij}^2 + Y_{ij}^2 + Z_{ij}^2), \quad (10)$$

where $X_{ij} = x_j - x_i$, $Y_{ij} = y_j - y_i$, $Z_{ij} = z_j - z_i$ are the difference variables between the population densities in patches i and j. We notice that both the averaged x, y, z-coupled network (3) and the corresponding stochastic network (2) are assumed to have the same Lyapunov function, so we will differentiate between the two of them using W_Φ and W_F for the averaged and stochastic networks, respectively. To facilitate cross-paper reading [Hasler *et al.*, 2013a, 2013b], we use the same notation for the Lyapunov function as well as for all other constants and bounds. Clearly, the zero of the Lyapunov function W_Φ corresponds to complete synchronization in the averaged network. At the same time, the trajectories of the stochastic network can only reach a neighborhood of the ghost synchronization solution in the stochastic network, therefore the Lyapunov function W_F cannot converge to zero, yet can become small. Governed by the stochastic switching, this Lyapunov function may increase temporarily, but the general tendency is to decrease. Therefore, the bounds of the sufficiently fast switching will have a probabilistic flavor.

The calculations of the probabilistic bounds are spatially cumbersome, therefore for clarity, we present a bound for the two-cell stochastic network (2) and its averaged analog (3) with the Lyapunov function (10) and $n = 2$. The two-cell stochastic network helps better isolate the robust effect of synchronization as a result of stochastic switching as the network becomes and stays completely uncoupled for a large fraction of time when the probability of switching p is small. At the same time, the larger n-patch network can remain connected or have at least most of the patches connected during a switching event (see Fig. 2). The extension of the rigorous bound to the n-patch network (2) is straightforward and can be performed, similarly to a switching network of n chaotic Lorenz oscillators [Jeter & Belykh, 2015].

Theorem 2. *Assume that the coupling strength $\varepsilon = \varepsilon_x = \varepsilon_y = \varepsilon_z$ is sufficiently strong, i.e. greater than the bound given in (4), such that synchronization in*

the two-patch averaged x, y, z-coupled network (3) is globally stable. Assume that the switching period τ is small enough to satisfy

$$\tau < \tau^*, \tag{11}$$

where the bound τ^* is given in (A.18) (see the Appendix). Then, the trajectory of the two-patch stochastic x, y, z-coupled network (2) almost surely reaches the U_0-neighborhood of the ghost synchronization solution, in finite time. Therefore, the stochastic x, y, z-coupled network converges to approximate synchronization globally and almost surely. The size of the U_0-neighborhood is defined by the level of the Lyapunov function W_Φ (11) ($n = 2$) such that $U_0 = V_0 + C_1$, where $V_0 = \frac{3}{2}\delta^2$ is the level of W_Φ with uniform synchronization mismatch $X_{12} = Y_{12} = Z_{12} = \delta$ and constant C_1 is given in (A.16). The constant δ in (A.17) controls the size of the U_0-neighborhood (i.e. the desired synchronization mismatch) and can be chosen arbitrarily small.

Proof. This theorem directly follows from the conditions of the general theorem, Theorem 9.1, given in [Hasler *et al.*, 2013b] and applied to the Lyapunov functions W_Φ and W_F (10) with $n = 2$ and their bounds on the first and second time derivatives, calculated along solutions of the averaged (3) and stochastic (2) networks. The details of their calculations are given in the Appendix. ■

Remark 1. The bound (11)–(A.18) is conservative as it comes from the application of Lyapunov functions and large deviation bounds [Hasler *et al.*, 2013b]. However, it explicitly relates the sufficient switching period τ with the probability p and strength of switching connections ε, the precision of synchronization δ, the size of the absorbing domain ψ, and the intrinsic parameters on the individual patch model. In particular, it suggests that the carrying capacity K and growth rate r of the producer, being the leading terms in (A.18), are destabilizing factors for promoting synchrony in the switching network as their increase lowers the bound τ^* and requires faster switching to maintain spatial synchronization.

Remark 2. The bound (11)–(A.18) guarantees a few things that are not immediately clear. It shows that if the switching rate is fast enough, the stochastic system will not just asymptotically converge to the U_0-neighborhood, but converge in a finite amount of time. It also guarantees globally stable synchronization in the switching x, y, z-coupled network (2) even if the probability of switching p is very small and the network is decoupled most of the time.

3.5. *Numerics*

We present numerically calculated bounds on τ to isolate the real window of switching periods τ, corresponding to approximate synchronization. As an example, we consider the two-patch x, y, z-coupled network (2) switching on and off with probability $p = 1/2$. The intrinsic parameter $a_1 = 4.99$ and $\Delta a = 0.04$ are such that the individual patch system switches between $a_1 = 4.99$ and $a_1 + p\Delta = 5.01$, both corresponding to chaotic dynamics. The averaged individual system is the model (1) with $a_1 = 5$, being the mean value of the two parameter values. The other switching parameters, s_{ij}, turn on and off stochastically, according to the process that we laid out in Sec. 2. Note that s_{ij} and a_1 switch with separate identically and independently distributed stochastic processes both with the probability of an "on" connection given by $p = \frac{1}{2}$. To test how the theory holds up, we pick a coupling strength such that the average coupling is slightly stronger than the synchronization threshold, representing a challenging case for the onset of synchronization in the stochastic network. If switching is fast enough, we expect that the network synchronizes, whereas if switching is not fast enough, we expect to see asynchrony. In Fig. 4, we observe exactly what we expect to see from the theory. As

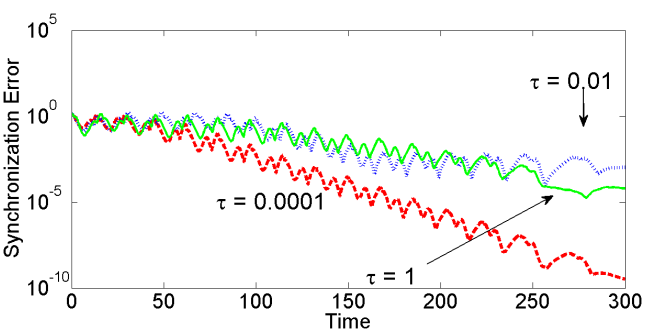

Fig. 4. The effect of the switching period τ on synchronization in the two-patch (x, y, z)-coupled stochastic network. The synchronization error corresponding to three switching periods, $\tau = 0.0001$ (red, dashed curve), $\tau = 0.01$ (blue, dotted curve), and $\tau = 1$ (solid, green curve). Nonzero size oscillations in the neighborhood of the ghost synchronization solution are due to stochastic parameter mismatch. The coupling strength $\varepsilon = 0.005$.

switching is fast ($\tau = 0.0001$), the system tends to synchrony (this is shown by the red, dashed curve). Slower switching at $\tau = 0.01$ and $\tau = 1$ does not provide the desired synchronization accuracy. We also notice that as switching becomes less fast, our intuition about the behavior of the network is less and less reliable, because slower switching periods can tend to synchrony more quickly than faster switching periods when switching is not fast (compare the green ($\tau = 1$) and blue ($\tau = 0.01$) curves where the slower switching with $\tau = 1$ provides smaller synchronization errors for these particular switching sequences).

4. Non-Fast Switching

While the above considered x, y, z-coupled network desynchronizes when the switching is not sufficiently fast, z-coupled stochastic networks (2) yield a highly nontrivial synchronizing effect. This migration coupling scheme where only predators are allowed to migrate (coupling through the z-variable only) has synchronization properties distinct from those of x-, y- and x, y, z-coupled networks. This is the only migration scheme which has a *bounded* range of coupling ε, where synchronization remains stable (see a well in its stability diagrams in Fig. 3). As a result, a stronger coupling, pushing the network out of the stability well, destabilizes synchronization. It is important to notice that the z-coupled networks of Rosenzweig–MacArthur prey–predator models demonstrate only locally stable synchronization within the stability well and global synchronization cannot be achieved for any coupling. Therefore, the rigorous theory of global convergence to synchronization in fast switching networks cannot be used for this network.

We choose the coupling strength $\varepsilon_z = \varepsilon = 0.35$ in the two-node z-coupled network, switching on and off with probability $p = \frac{1}{2}$. When turned on, this excessively strong coupling corresponds to a nonsynchronized state of the network. When the coupling is turned off, the network is decoupled and cannot be synchronized. It is worth noticing that synchronization in the averaged network is also unstable as the mean coupling value $p\varepsilon = 0.175$,

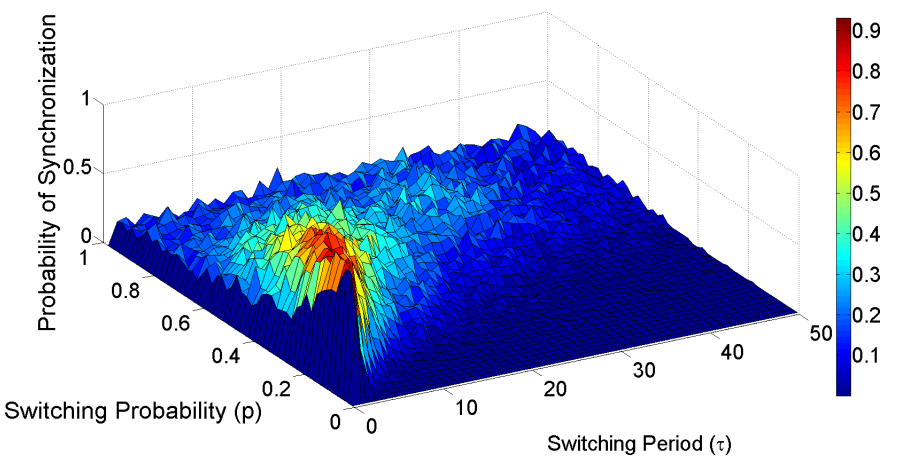

(a)

Fig. 5. (a) Probability of approximate synchronization in the two-patch z-coupled network as a function of the switching probability p and the switching period τ. The colors mirror the values on the z-axis, with red (lighter colors) corresponding to higher probability of convergence (with dark red at probability 1) and blue (darker colors) corresponding to lower probabilities (dark blue at probability 0). The coupling in the averaged network is fixed at $p\varepsilon = 0.175$, marked by • in Fig. 3, to be outside the stability well. As the probability p changes, the coupling strength ε in the stochastic network is adjusted to keep $p\varepsilon = 0.175$ unchanged. When switching is fast and the switching period τ is close to zero, the probability of synchronization is zero as the switching network behaves similarly to the unstable averaged network. Notice the large bump on the irregular surface indicating the emergence of approximate synchronization in a window of non-fast switching periods. (b) Various cross-sections from the surface above. When p is small, such as for $p = 0.1$ (blue, dotted curve) and $p = 0.25$ (red, dashed curve), there are narrow windows for intermediate switching for which approximate synchronization is stable with high probability. For $p = 0.5$ (black curve), there is a trade-off between high probability of approximate synchronization and the length of the window for τ. Switching probability around $p = 1/2$ yields the largest stability window. When p is large, such as for $p = 0.75$ (green dotted curve), and $p = 0.9$ (magenta curve), the network does not converge to approximate synchronization consistently for any value of τ. Probability calculations are based on 100 trials.

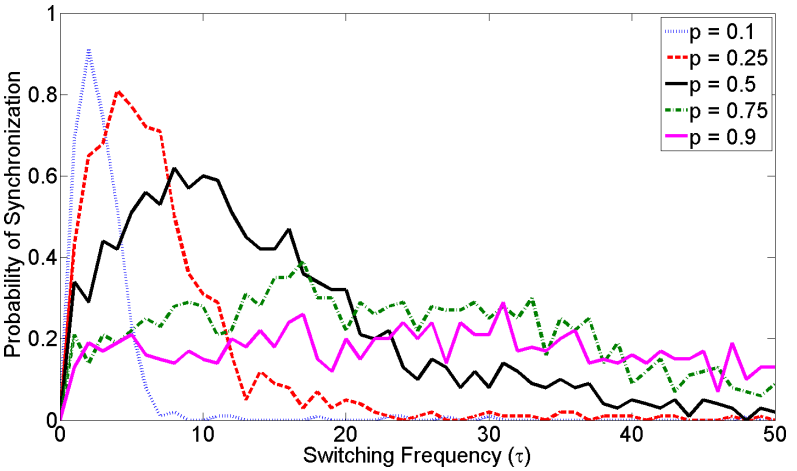

(b)

Fig. 5. (*Continued*)

marked by a solid circle in Fig. 3, is outside its stability well. Thus, the network switches between two nonsynchronous dynamics; when the switching is fast and its dynamics becomes close to those of the averaged network, synchronization in the network is unstable, as expected. However, we find a window of intermediate switching periods ($5 < \tau < 20$) in which approximate synchronization becomes stable with high probability, against all odds (see Fig. 5). To give the reader a sense of how these switching periods relate to the characteristic period of the individual patch's ecological cycle $T \approx 200$, we present the window of their ratio: $\frac{1}{40} < \frac{\tau}{T} < \frac{1}{10}$, suggesting that the coupling between the patches must be activated at least as many as ten and as fewer as 40 times during the ecological cycle for stable approximate synchronization to emerge from switching between two nonsynchronous dynamics. Figure 5 also shows that the probability $p = \frac{1}{2}$ yields the largest window of synchronization and suggests the importance of the most probable reswitching between the nonsynchronous dynamics to maximize the stabilization effect.

We previously named regions of dynamical stabilization, induced by stochastic switching, "windows of opportunity," to further emphasize that there are consistently favorable conditions in which the stochastic and deterministic parameters of a switching system match up appropriately [Belykh *et al.*, 2013; Jeter & Belykh, 2015] to induce an otherwise unexpected effect. To some extent, one can draw some parallels between the stabilization of approximate synchronization in the non-fast switching network (2) with stochastic resonance [Benzi *et al.*, 1981; Wiesenfeld & Moss, 1995] where stochasticity makes the time scales of a periodic driving force and driving noise match each other and pushes subthreshold oscillations beyond a threshold level. However, the two phenomena have completely different dynamical origins.

5. Conclusions

We have proposed a switching "blinking" network of tritrophic food-chain models as a realistic description of ecological networks where migration episodes are due to short-term meteorological conditions; however, the migration occurs relatively frequently during the characteristic period of the ecological cycle. We have shown how the recently developed theory [Hasler *et al.*, 2013a, 2013b] of general fast switching dynamical systems can be used to study metapopulation synchronization. Following [Belykh *et al.*, 2009], we have shown that the dispersal of all the species is much more effective than those of one trophic level in promoting synchronized dynamics. We used this three-species dispersal case to derive explicit probabilistic bounds on the switching frequency sufficient for the switching stochastic network to synchronize almost surely and globally.

Going beyond fast switching, we considered a switching network where only the predator population can migrate and discovered a large window of intermediate switching periods in which synchronization in the switching network becomes stable even though it is unstable in the averaged/fast-switching network. In this case, the network

switches between two nonsynchronous states; one corresponds to the uncoupled network, whereas the other is determined by a network topology with overly strong desynchronizing dispersal. Yet, the network can synchronize in this "resonant" window of intermediate switching periods with high probability. In this context, the sporadic stochastic switching plays a constructive role in stabilizing metapopulation synchrony and indicates the importance of reswitching between the unstable states. At the same time, metapopulation synchrony increases the probability of extinction as all patches synchronously follow the same ecological cycle with typical outbreaks and crashes such that one patch in an endangered state cannot be saved by the migration from another equally endangered patch. In this respect, the role of stochasticity in the switching ecological network can be viewed as destructive as it decreases overall metapopulation persistence. Remarkably, the opposite examples of stochastic dispersal are available [Williams & Hastings, 2013] where switching between two sets of dynamics, each of which leads to extinction, can promote persistence of marine organisms' metapopulations. However, the models and type of stochastic dispersal used in this study [Williams & Hastings, 2013] are quite different from ours. The effect of nonfast switching between stable two-dimensional linear systems has previously been studied. It was shown that switching between two stable linear nodes can cause the trajectory to escape to infinity when the switching is not fast [Lawley *et al.*, 2014].

We have chosen identically distributed independent random variables as the driving stochastic process for the migration in the ecological network. As a result, migration episodes occur independently from each other. As the migration episodes are often governed by meteorological conditions that could be driven by a Markov process, the extension of this study to ecological networks where the probability of a migration episode depends on the present migration connections is an important research topic. Outside of Ecology, on–off switching networks represent a class of evolving dynamical networks [Belykh *et al.*, 2014], changing their structure stochastically or in accordance with some governing deterministic rule. Epileptic brain networks switching their functional topology during epileptic seizures [Lehnertz *et al.*, 2014] are an important example.

Acknowledgments

This work was supported by the National Science Foundation under Grant No. DMS-1009744, the US ARO Network Program under grant W911NF-15-1-0267, and GSU Brains & Behavior program. We are grateful to Martin Hasler and Sergio Rinaldi for helpful discussions.

References

Belykh, I. V., Belykh, V. N. & Hasler, M. [2005a] "Blinking model and synchronization in small-world networks with a time-varying coupling," *Physica D* **195**, 188–206.

Belykh, V. N., Belykh, I. V. & Hasler, M. [2005b] "Connection graph stability method for synchronized coupled chaotic systems," *Physica D* **195**, 159–187.

Belykh, I., Piccardi, C. & Rinaldi, S. [2009] "Synchrony in tritrophic food chain metacommunities," *J. Biol. Dyn.* **3**, 497–514.

Belykh, I., Belykh, V. N., Jeter, R. & Hasler, M. [2013] "Multistable randomly switching oscillators: The odds of meeting a ghost," *Eur. Phys. J. Spec. Topics* **222**, 2497–2507.

Belykh, I., di Bernardo, M., Kurths, J. & Porfiri, M. [2014] "Evolving dynamical networks," *Physica D* **267**, 1–6.

Benzi, R., Sutera, A. & Vulpani, A. [1981] "The mechanism of stochastic resonance," *J. Phys. A*: *Math. Gen.* **14**, L453–L457.

Blasius, B., Huppert, A. & Stone, L. [1999] "Complex dynamics and phase synchronization in spatially extended ecological systems," *Nature* **399**, 354–359.

Cantrell, R. S., Cosner, C. & Ruan, S. (eds.) [2009] *Spatial Ecology* (CRC-Chapman & Hall, Boca Raton).

Cattadori, I. M., Hudson, P. J., Merler, S. & Rizzoli, A. [1999] "Synchrony, scale and temporal dynamics of rock partridge (Alectoris graeca saxatilis) populations in the dolomites," *J. Anim. Ecol.* **68**, 540–549.

Cazelles, B. & Boudjema, G. [2001] "The Moran effect and phase synchronization in complex spatial community dynamics," *Amer. Natur.* **157**, 670–676.

Chave, J. [2013] "The problem of pattern and scale in ecology: What have we learned in 20 years?" *Ecol. Lett.* **16**, 4–16.

Colombo, A., Dercole, F. & Rinaldi, S. [2008] "Remarks on metacommunity synchronization with application to prey–predator systems," *Amer. Natur.* **171**, 430–442.

De Lellis, P., di Bernardo, M., Garofalo, F. & Porfiri, M. [2010] "Evolution of complex networks via edge snapping," *IEEE Trans. Circuits Syst.-I* **57**, 2132–2143.

Deng, B. & Hines, G. [2001] "Food chain chaos due to Shilnikov's orbit," *Chaos* **12**, 533–538.

Earn, D., Levin, S. & Rohani, P. [2000] "Coherence and conservation," *Science* **270**, 1360–1364.

Elton, C. S. [1924] "Periodic fluctuations in the numbers of animals," *British J. Exper. Biol.* **2**, 119–163.

Elton, C. S. & Nicholson, M. [1942] "The ten-year cycle in numbers of the lynx in Canada," *J. Anim. Ecol.* **11**, 215–244.

Frasca, M., Buscarino, A., Rizzo, A., Fortuna, L. & Boccaletti, S. [2008] "Synchronization of moving chaotic agents," *Phys. Rev. Lett.* **100**, 044102.

Grenfell, B. T., Wilson, K., Finkenstädt, B. F., Coulson, T. N., Murray, S., Albon, S. D., Pemberton, J. M., Clutton-Brock, T. H. & Crawley, M. J. [1998] "Noise and determinism in synchronized sheep dynamics," *Nature* **394**, 674–677.

Hanski, I. & Woiwod, I. P. [1993] "Spatial synchrony in the dynamics of moth and aphid populations," *J. Anim. Ecol.* **62**, 656–668.

Hasler, M. & Belykh, I. [2005] "Blinking long-range connections increase the functionality of locally connected networks," *IEICE Trans. Fund.* **E88-A**, 2647–2655.

Hasler, M., Belykh, V. N. & Belykh, I. [2013a] "Dynamics of stochastically blinking systems. Part I: Finite time properties," *SIAM J. Appl. Dyn. Syst.* **12**, 1007–1030.

Hasler, M., Belykh, V. N. & Belykh, I. [2013b] "Dynamics of stochastically blinking systems. Part II: Asymptotic properties," *SIAM J. Appl. Dyn. Syst.* **12**, 1031–1084.

He, D., Stone, L. & Cazelles, B. [2010] "Noise-induced synchronization in multitrophic chaotic ecological systems," *Int. J. Bifurcation and Chaos* **20**, 1779.

Higgins, K., Hastings, A., Sarvela, J. N. & Bostford, L. W. [1997] "Stochastic dynamics and deterministic skeletons: Population behavior of Dungeness crab," *Science* **276**, 1431–1435.

Huang, Y. & Diekmann, O. [2001] "Predator migration in response to prey density: What are the consequences?" *J. Math. Biol.* **43**, 561–581.

Jeter, R. & Belykh, I. [2015] "Synchronization in on-off stochastic networks: Windows of opportunity," *IEEE Trans. Circuits Syst.-I* **62**, 1260–1269.

Johnson, D. M., Liebhold, A. M., Bjørnstad, O. N. & McManus, M. L. [2005] "Circumpolar variation in periodicity and synchrony among gypsy moth populations," *J. Anim. Ecol.* **74**, 882–892.

Kuznetsov, Yu. A., De Feo, O. & Rinaldi, S. [2001] "Belyakov homoclinic bifurcations in a tritrophic food chain model," *SIAM J. Appl. Math.* **62**, 462–487.

Lawley, S. D., Mattingly, J. C. & Reed, M. C. [2014] "Sensitivity to switching rates in stochastically switched ODEs," *Commun. Math. Sci.* **12**, 1343–1352.

Lehnertz, K., Ansmanna, G., Bialonski, S., Dickten, H., Geier, C. & Porz, S. [2014] "Evolving networks in the human epileptic brain," *Physica D* **267**, 7–15.

Levin, S. [1992] "The problem of pattern and scale in ecology," *Ecology* **73**, 1943–1967.

Lü, J. & Chen, G. [2005] "A time-varyng complex dynamical network model and its controlled synchronization network," *IEEE Trans. Automat. Contr.* **50**, 841–846.

Pecora, L. M. & Carroll, T. L. [1998] "Master stability functions for synchronized coupled systems," *Phys. Rev. Lett.* **80**, 2109–2112.

Porfiri, M., Stilwell, D. J., Bollt, E. M. & Skufca, J. D. [2006] "Random talk: Random walk and synchronizability in a moving neighborhood network," *Physica D* **224**, 102–113.

Ranta, E., Kaitala, V., Lindström, J. & Lindén, H. [1995] "Synchrony in population dynamics," *Proc. Roy. Soc. Lond. B* **262**, 113–118.

Ranta, E., Kaitala, V., Lindström, J. & Helle, E. [1997] "The Moran effect and synchrony in population dynamics," *Oikos* **78**, 136–142.

Ravera, O. [1977] "Caratteristiche chimiche e fisiche delle acque del lago di lugano," *Quaderni di Geologia e Geofisica Applicata* **2**, 137–148.

Rinaldi, S. [2009] "Synchrony in slow-fast metapopulations," *Int. J. Bifurcation and Chaos* **19**, 2447–2453.

Rinaldi, S. [2012] "Recurrent and synchronous insect pest outbreaks in forests," *Theor. Popul. Biol.* **81**, 1–8.

Rosenzweig, M. L. & MacArthur, R. H. [1963] "Graphical representation and stability conditions of predator–prey interactions," *Amer. Natur.* **97**, 209–223.

Schwartz, M. K., Mills, L. S., McKelvey, K. S., Ruggiero, L. F. & Allendorf, F. W. [2002] "DNA reveals high dispersal synchronizing the population dynamics of Canadian lynx," *Nature* **415**, 520–522.

So, P., Cotton, B. & Barreto, E. [2008] "Synchronization in interacting populations of heterogeneous oscillators with time-varying coupling," *Chaos* **18**, 037114.

Sorrentino, F. & Ott, E. [2008] "Adaptive synchronization of dynamics on evolving complex networks," *Phys. Rev. Lett.* **100**, 114101.

Wiesenfeld, K. & Moss, F. [1995] "Stochastic resonance and the benefits of noise: From ice ages to crayfish and SQUIDs," *Nature* **373**, 33–36.

Williams, P. D. & Hastings, A. [2013] "Stochastic dispersal and population persistence in marine organisms," *Amer. Natur.* **182**, 271–282.

Appendix

Derivation of the Bound from Theorem 2

In this appendix, we present the calculations of the constants used in the statement of Theorem 2. As we consider the two-patch network, we can rewrite the Lyapunov function (10) for the different variables $X = x_2 - x_1$, $Y = y_2 - y_1$, $Z = z_2 - z_1$ as

$$W = \frac{1}{2}(X^2 + Y^2 + Z^2). \tag{A.1}$$

To apply Theorem 9.1 [Hasler *et al.*, 2013b] to the global stability of approximate synchronization in the two-patch x, y, z-coupled network (2) with $\varepsilon = \varepsilon_x = \varepsilon_y = \varepsilon_z$, we need to calculate upper bounds on the first and second time derivatives of the Lyapunov function W, calculated along solutions of the averaged and switching networks. As in the main text, we shall use the same notation for the Lyapunov functions and their derivatives as in [Hasler *et al.*, 2013b]. The required derivatives are

$$\begin{aligned} B_{W\Phi} &= \max_{\mathbf{x}\in\mathbf{R}} |D_\Phi W(\mathbf{x})| \\ LB_{W\Phi} &= \max_{\mathbf{x}\in\mathbf{R}} |D_\Phi^2 W(\mathbf{x})| \\ B_{WF} &= \max_{\mathbf{s}\in 0,1^M} \max_{x\in\mathbf{R}} |D_F W(\mathbf{x},\mathbf{s})| \\ LB_{WF} &= \max_{\mathbf{s},\bar{\mathbf{s}}\in 0,1^M} \max_{x\in\mathbf{R}} |D_F^2 W(\mathbf{x},\bar{\mathbf{s}},\mathbf{s})|, \end{aligned} \tag{A.2}$$

where $\mathbf{x}$ is the vector of $\mathbf{x}_i = \{x_i, y_i, z_i\}, i = 1, 2$, $\mathbf{R}$ is the systems' absorbing domain, $\mathbf{s}$ is a set of stochastic sequences corresponding to the connections between patches and the switching of the parameter a_1; similarly, $\bar{\mathbf{s}}$ corresponds to another set of stochastic switching sequences. We start with $B_{W\Phi}$, which requires the first time derivative of the Lyapunov function of the averaged system:

$$D_\Phi W(x) = X\dot{X} + Y\dot{Y} + Z\dot{Z}.$$

Here, the derivatives $\dot{X}$, $\dot{Y}$, and $\dot{Z}$ are given by the following difference system, obtained by subtracting the corresponding equations of the averaged network

$$\begin{aligned} \dot{X} &= [(f(x_2) - f(x_1)) - (g(x_2)y_2 - g(x_1)y_1)] \\ &\quad - 2p\varepsilon X \\ \dot{Y} &= [(g(x_2)y_2 - g(x_1)y_1) - (h(y_2)z_2 - h(y_1)z_1)] \\ &\quad - (m_1 + 2p\varepsilon)Y \\ \dot{Z} &= [h(y_2)z_2 - h(y_1)z_1] - (m_2 + 2p\varepsilon)Z \end{aligned} \tag{A.3}$$

with $f(\eta) = r\eta(1 - \frac{\eta}{K})$, $g(\eta) = \frac{a_1^*\eta}{1+a_1^* b_1 \eta}$, where $\eta = x_1, x_2$ and $a_1^* = [1 + \Delta a \cdot p]a_1$ and $h(\xi) = \frac{a_2\xi}{1+a_2 b_2 \xi}$ with $\xi = y_1, y_2$.

Recall that $0 \le x_i,\ y_i,\ z_i < \psi = \frac{K}{4rm_2}(r + m_2)^2$ [cf. (9)]. We use this bound to find $B_{W\Phi} = \max_{\mathbf{x}\in\mathbf{R}} |D_\Phi W(\mathbf{x})|$ by substituting either 0 or ψ for each $x_i,\ y_i,\ z_i$ $(i = 1, 2)$, depending on which will maximize each term. While this may not give the tightest bound, it simplifies the derivation of the bound, and makes the final bound a little more manageable:

$$\begin{aligned} &\max|D_\Phi W(x)| \\ &\quad = \left[\psi\left(r\psi + p\varepsilon\psi + \frac{r\psi^2}{K} + a_1^*\psi + p\varepsilon\psi\right)\right. \\ &\qquad + \psi(a_1^*\psi^2 + p\varepsilon\psi + m_1\psi + a_2\psi^2 + p\varepsilon\psi) \\ &\qquad \left. + \psi(a_2\psi^2 + p\varepsilon\psi + m_2\psi + p\varepsilon\psi)\right], \end{aligned}$$

which reduces to

$$\begin{aligned} B_{W\Phi} = \psi^2 \Bigg(&r + \frac{r\psi}{K} + 2a_1^*\psi \\ &+ m_1 + 2a_2\psi + m_2 + 6p\varepsilon\Bigg). \end{aligned} \tag{A.4}$$

Next, we repeat this process for $LB_{W\Phi} = \max_{\mathbf{x}\in\mathbf{R}} |D_\Phi^2 W(\mathbf{x})|$ which requires the second time derivative of the Lyapunov function of the averaged system, $D_\Phi^2 W(\mathbf{x})$. Taking the second time derivative of W_Φ, we get:

$$D_\Phi^2 W(\mathbf{x}) = \dot{X}^2 + X\ddot{X} + \dot{Y}^2 + Y\ddot{Y} + \dot{Z}^2 + Z\ddot{Z},$$

where $\ddot{X}$, $\ddot{Y}$, and $\ddot{Z}$ are defined by the system

$$\begin{aligned} \ddot{X} &= [\dot{f}(x_2) - \dot{f}(x_1)] - [\dot{g}(x_2)y_2 + g(x_2)\dot{y}_2 \\ &\quad - \dot{g}(x_1)y_1 - g(x_1)\dot{y}_1] - 2p\varepsilon\dot{X} \\ \ddot{Y} &= [\dot{g}(x_2)y_2 + g(x_2)\dot{y}_2 - \dot{g}(x_1)y_1 - g(x_1)\dot{y}_1] \\ &\quad - [\dot{h}(y_2)z_2 + h(y_2)\dot{z}_2 - \dot{h}(y_1)z_1 - h(y_1)\dot{z}_1] \\ &\quad - (m_1 + 2p\varepsilon)\dot{Y} \end{aligned}$$

$$\ddot{Z} = \dot{h}(y_2)z_2 + h(y_2)\dot{z}_2 - \dot{h}(y_1)z_1 - h(y_1)\dot{z}_1 - (m_2 + 2p\varepsilon)\dot{Z}. \tag{A.5}$$

Then, using the same methods as before, we replace all of the variables with either ψ or 0, depending on which helps maximize the equation term by term. Using *Mathematica*, we simplify the tedious expression to get:

$$\begin{aligned} LB_{W\Phi} &= \max|D^2_{\Phi}W(\mathbf{x})| \\ &= \psi^2\Bigg[4(a_1^*)^2\psi^2 + 6a_2^2\psi^2 + 2m_1^2 + m_2 \\ &\quad + 2m_2^2 + 2p\varepsilon + 7pm_1\varepsilon + 5p\varepsilon m_2 \\ &\quad + 20p^2\varepsilon^2 + a_2\psi(1 + 5m_1 + a_1^*\psi(4 + m_1) \\ &\quad + 4m_2 + 17p\varepsilon + m_1p\varepsilon) + 6\frac{r\varepsilon\psi}{K} + 6p\varepsilon r \\ &\quad + 2p\varepsilon\psi r + 3\frac{\psi^2r^2}{K} + 2\frac{\psi r^2}{K} + r^2 \\ &\quad + \frac{a_1^*\psi}{K}(3Km_1 + 16p\varepsilon K + 5\psi r + 3Kr)\Bigg]. \end{aligned} \tag{A.6}$$

After finding these bounds for the averaged network, we must do the same thing for the stochastic system. We start by finding

$$\max|D_FW(\mathbf{x},\mathbf{s})| = X\dot{X} + Y\dot{Y} + Z\dot{Z},$$

where the derivatives $\dot{X}$, $\dot{Y}$, and $\dot{Z}$ are governed by the difference system which is identical to (A.5), when p is replaced with $s_{12}(t)$ and a_1^* with $[1 + \Delta a \cdot \xi_1]a_1$ and a_1^* with $[1 + \Delta a \cdot \xi_2]a_1$ in the functions $g(x_1)$ and $g(x_2)$, respectively. Similarly to the calculations of $B_{W\Phi}$, the expression for $\max|D_FW(\mathbf{x},\mathbf{s})|$ can be simplified using the same bounds. It is worth mentioning that in choosing the favorable bound term by term, the inequalities will be maximized for $s_{12} = 1$, i.e. when the switch is "on" and $\xi_1 = \xi_2 = 1$ such that

$$\begin{aligned} B_{WF} &= \max|D_FW(\mathbf{x},\mathbf{s})| \\ &= \Bigg[\psi\left(r\psi + \varepsilon\psi + \frac{r\psi^2}{K} + \hat{a}_1\psi + \varepsilon\psi\right) \\ &\quad + \psi(\hat{a}_1\psi^2 + \varepsilon\psi + m_1\psi + a_2\psi^2 + \varepsilon\psi) \\ &\quad + \psi(a_2\psi^2 + \varepsilon\psi + m_2\psi + \varepsilon\psi)\Bigg], \end{aligned}$$

where $\hat{a}_1 = [1 + \Delta a]a_1$. The bound further reduces as follows

$$B_{WF} = \psi^2\left(r + \frac{r\psi}{K} + 2\hat{a}_1\psi + m_1 + 2a_2\psi + m_2 + 6\varepsilon\right). \tag{A.7}$$

Then, we take the second time derivative of W_F to get

$$D^2_FW(\mathbf{x},\mathbf{s},\bar{\mathbf{s}}) = \dot{X}^2 + X\ddot{X} + \dot{Y}^2 + Y\ddot{Y} + \dot{Z}^2 + Z\ddot{Z},$$

with $\ddot{X}$, $\ddot{Y}$, and $\ddot{Z}$ defined in difference system (A.5), when p is replaced with $\bar{s}_{12}(t)$ and a_1^* with $[1 + \Delta a \cdot \bar{\xi}_1]a_1$ and a_1^* with $[1 + \Delta a \cdot \bar{\xi}_2]a_1$ in the functions $g(x_1)$ and $g(x_2)$, respectively. The reader should notice the additional stochastic variables $\bar{s}_{12}$, $\bar{\xi}_1$, and $\bar{\xi}_2$. This is another realization of the stochastic sequence that does not match the realization given by s_{12}, ξ_1, and ξ_2. However, after substituting the bounds on the state variables, we observe that the maximum is obtained when $s_{12} = \bar{s}_{12} = 1$, $\xi_1 = \bar{\xi}_1 = 1$, and $\xi_2 = \bar{\xi}_2 = 1$. Therefore, the bound simplifies to

$$\begin{aligned} LB_{WF} &= \max|D^2_FW(x)| \\ &= \psi^2\Bigg[4\hat{a}_1^2\psi^2 + 6a_2^2\psi^2 + 2\varepsilon + 20\varepsilon^2 \\ &\quad + 7\varepsilon m_1 + 2m_1^2 + m_2 + 5\varepsilon m_2 + 2m_2^2 \\ &\quad + a_2\psi\cdot(1 + 5m_1 + \hat{a}_1\psi(4 + m_1) \\ &\quad + \varepsilon(17 + m_1) + 4m_2) + 6\frac{\psi\varepsilon r}{K} \\ &\quad + 6\varepsilon r + 2\psi\varepsilon r + 3\frac{\psi^2r^2}{K^2} + 2\frac{\psi r^2}{K} + r^2 \\ &\quad + \frac{\hat{a}_1\psi}{K}\cdot(16\varepsilon K + 5\psi r + 3K(m_1 + r))\Bigg]. \end{aligned} \tag{A.8}$$

The next step in deriving the bound τ^* of Theorem 2 is to define the size of the δ-neighborhood of the ghost synchronization solution of the stochastic system (2). To do this, we choose a level curve of the Lyapunov function W_Φ for the averaged system (3):

$$V_0 : W = \frac{1}{2}(\delta_X^2 + \delta_Y^2 + \delta_Z^2). \tag{A.9}$$

We let $\delta = \max\{\delta_X, \delta_Y, \delta_Z\}$, which simplifies the level to

$$V_0 : W_\Phi \leq \frac{3}{2}\delta^2. \tag{A.10}$$

We define another level, V_1 as the absorbing domain of the Lyapunov function, which we obtain by replacing each difference variable with its maximum value, subject to the constraints on $\mathbf{x}$. We get:

$$V_1 : W_\Phi = \frac{1}{2}(\psi^2 + \psi^2 + \psi^2) = \frac{3}{2}\psi^2. \tag{A.11}$$

These level curves allow us to define the following quantity used in the general Theorem 9.1 [Hasler *et al.*, 2013b]:

$$\gamma = \min_{\mathbf{x}\in\mathbf{R}, V_0 \leq W_\Phi \leq V_1} |D_\Phi W(x)|.$$

We can see that $|D_\Phi W(X)|$ is minimized at the level V_0, which corresponds to the δ-neighborhood. Hence, we calculate γ as:

$$\begin{aligned}\gamma &= \min_{\mathbf{x}\in\mathbf{R}, V_0 \leq W_\Phi \leq V_1} |D_\Phi W(x)| \\ &= \left|\delta^2\left(r - \frac{r}{K}\delta - m_1 - m_2 - 6p\varepsilon\right)\right|. \end{aligned}\tag{A.12}$$

We must also define the following constants that are used in the theorem:

$$\begin{aligned} c &= \frac{1}{64(LB_{WF} + LB_{W\Phi})B_{WF}^2} \\ D &= 8(LB_{WF} + LB_{W\Phi}) \\ U_0 &= \left\{x \,|\, W(x) < V_0 + \frac{4\gamma^2}{D}\right\}, \end{aligned}\tag{A.13}$$

where U_0 is a neighborhood of the synchronization solution of the averaged system (3), and is slightly larger than V_0, which corresponds to the δ-neighborhood of the ghost synchronization solution in the stochastic system (2). After substituting the values for B_{WF}, LB_{WF}, and $LB_{W\Phi}$ we obtain

$$\begin{aligned} c = K^4 \cdot \Bigg[& 64\psi^4(2\hat{a}_1\psi K + 2a_2\psi K + Km_1 + Km_2 + 6Kp\varepsilon + \psi r + Kr)^2 \\ & \times \Bigg(\frac{1}{K^2\psi^2}(6a_2^2\psi^2K^2 + 4(\hat{a}_1)^2\psi^2K^2 + 2K^2m_1^2 + K^2m_2 + 2K^2m_2^2 + 2p\varepsilon K^2 + 7p\varepsilon K^2m_1 \\ & + 5p\varepsilon K^2m_2 + 20p^2\varepsilon^2K^2 + a_2\psi K^2(15m_1 + \hat{a}_1\psi(4 + m_1) + 4m_2 + 17p\varepsilon + p\varepsilon m_1) + 6\psi pKr\varepsilon \\ & + 6p\varepsilon K^2r + 2\psi p\varepsilon rK^2 + 3\psi^2r^2 + 2\psi r^2K + K^2r^2 + \hat{a}_1\psi K(3Km_1 + 16p\varepsilon K + 5\psi r + 3Kr)) \\ & + \frac{1}{K^2\psi^2}(6a_2^2\psi^2K^2 + a_2\psi K^2(1 + 4m_2 + 4a_1^*\psi + 17p\varepsilon + m_1 \cdot (5 + a_1^*\psi + p\varepsilon)) + 3\psi^2r^2 \\ & + \psi Kr(5a_1^*\psi + 6p\varepsilon + 2r) + K^2(2m_1^2 + m_2 + 2m_2^2 + 2p\varepsilon + 3a_1^*\psi m_1 + 7p\varepsilon m_1 \\ & + 5p\varepsilon m_2 + 4(a_1^*)^2\psi^2 + 16a_1^*\psi p\varepsilon + 20p^2\varepsilon^2 + 3a_1^*\psi r + 6rp\varepsilon + 2\psi rp\varepsilon + r^2))\Bigg)\Bigg]^{-1} \end{aligned}\tag{A.14}$$

and

$$\begin{aligned} D = {} & 8\psi^2(12a_2^2\psi^2 + 4(a_1^*)^2\psi^2 + 4\hat{a}_1^2\psi^2 + a_2\psi((\hat{a}_1\psi + a_1^*\psi)(4 + m_1) \\ & + 2(1 + 5m_1 + 4m_2 + 17p\varepsilon + m_1p\varepsilon))m_1p\varepsilon) + \frac{(a_1^* + \hat{a}_1)\psi}{K}(5\psi r + K(3m_1 + 16p\varepsilon + 3r)) \\ & + 2\left(\frac{1}{K}(3\psi^2r^2 + 2\psi Kr(3p\varepsilon + r) + 2m_1^2 + m_2 + 2m_2^2 + r^2 + p\varepsilon(2 + 7m_1 + 5m_2 + 20p\varepsilon + 6r + 2\psi r))\right). \end{aligned}\tag{A.15}$$

With C_1 being defined as $\frac{4\gamma}{D}$, we get

$$\begin{aligned} C_1 = \delta^4\left(r - \frac{r}{K}\delta - m_1 - m_2 - 6p\varepsilon\right)^2 \cdot \frac{1}{2}\Bigg[& \psi^2(12a_2^2\psi^2 + 4(a_1^*)^2\psi^2 + 4\hat{a}_1^2\psi^2 \\ & + a_2\psi((\hat{a}_1\psi + a_1^*\psi)(4 + m_1) + 2(1 + 5m_1 + 4m_2 + 17p\varepsilon + m_1p\varepsilon))) \end{aligned}$$

$$+\frac{(a_1^*+\hat{a}_1)\psi}{K}(5\psi r+K(3m_1+16p\varepsilon+3r))+2\left(\frac{1}{K}(3\psi^2r^2+2\psi Kr(3p\varepsilon+r)\right.$$
$$\left.+2m_1^2+m_2+2m_2^2+r^2+p\varepsilon(2+7m_1+5m_2+20p\varepsilon+6r+2\psi r))\right)\Bigg]^{-1}. \tag{A.16}$$

The desired bound on the switching period τ^* in Theorem 2 comes from the bound in Theorem 9.1 [Hasler *et al.*, 2013b] such that

$$\tau<\tau*=\frac{c\gamma^3}{\ln\left[D\dfrac{(V_1-V_0)}{\gamma^2}\right]}. \tag{A.17}$$

Plugging the constants c (A.14), γ (A.12), D (A.15), V_0 (A.10), V_1 (A.11) into the general expression (A.17) yields the final bound used in Theorem 2:

$$\begin{aligned}\tau<\tau*=K^4&\left|\delta^2\left(r-\frac{r}{K}\delta-m_1-m_2-6p\varepsilon\right)\right|^3\\
&\cdot\Bigg(64\psi^4(2\hat{a}_1\psi K+2a_2\psi K+Km_1+Km_2+6Kp\varepsilon+\psi r+Kr)^2\\
&\times\Bigg(\frac{1}{K^2\psi^2}(6a_2^2\psi^2K^2+4\hat{a}_1^2\psi^2K^2+2K^2m_1^2+K^2m_2+2K^2m_2^2+2p\varepsilon K^2+7p\varepsilon K^2m_1\\
&+5p\varepsilon K^2m_2+20p^2\varepsilon^2K^2+a_2\psi K^2(15m_1+\hat{a}_1\psi(4+m_1)+4m_2+17p\varepsilon+p\varepsilon m_1)+6\psi pKr\varepsilon\\
&+6p\varepsilon K^2r+2\psi p\varepsilon rK^2+3\psi^2r^2+2\psi r^2K+K^2r^2+\hat{a}_1\psi K(3Km_1+16p\varepsilon K+5\psi r+3Kr))\\
&+\frac{1}{K^2\psi^2}(6a_2^2\psi^2K^2+a_2\psi K^2(1+4m_2+4a_1^*\psi+17p\varepsilon+m_1(5+a_1^*\psi+p\varepsilon))\\
&+3\psi^2r^2+\psi Kr(5a_1^*\psi+6p\varepsilon+2r)+K^2(2m_1^2+m_2+2m_2^2+2p\varepsilon+3a_1^*\psi m_1\\
&+7p\varepsilon m_1+5p\varepsilon m_2+4(a_1^*)^2\psi^2+16a_1^*\psi p\varepsilon+20p^2\varepsilon^2+3a_1^*\psi r+6rp\varepsilon+2\psi rp\varepsilon+r^2))\Bigg)\Bigg)\\
&\times\ln\Bigg[8\psi^2\Bigg(12a_2^2\psi^2+4(a_1^*)^2\psi^2+4\hat{a}_1^2\psi^2+a_2\psi((a_1^*\psi+\hat{a}_1\psi)(4+m_1)+2(1+5m_1+4m_2\\
&+17p\varepsilon+m_1p\varepsilon))+\frac{(a_1^*+\hat{a}_1)\psi}{K}(5\psi r+K(3m_1+16p\varepsilon+3r))+2\left(\frac{1}{K}(3\psi^2r^2+2\psi Kr(3p\varepsilon+r)\right.\\
&\left.+2m_1^2+m_2+2m_2^2+r^2+p\varepsilon(2+7m_1+5m_2+20p\varepsilon+6r+2\psi r))\right)\\
&\times\frac{\dfrac{3}{2}(\psi^2-\delta)}{\delta^4\left(r-\dfrac{r}{K}\delta-m_1-m_2-6p\varepsilon\right)^2}\Bigg)\Bigg]^{-1},\end{aligned} \tag{A.18}$$

where once again $\psi = \frac{K}{4rm_2}(r+m_2)^2$ is the absorbing domain bounds [cf. (9)], $a_1^* = [1+\Delta a \cdot p]a_1$, and $\hat{a}_1 = [1+\Delta a]a_1$. Note that the bound τ^* is explicit in the parameters of the stochastic network. The size of the neighborhood U_0 used in Theorem 2 is given by $U_0 = V_0 + C_1$, where $V_0 = \frac{3}{2}\delta^2$ [cf. (A.10)] and C_1 is given in (A.16). The constant δ defines the required precision of synchronization and can be chosen arbitrarily.

This completes the calculation of the bounds that are necessary to apply general Theorem 9.1 [Hasler *et al.*, 2013b] on the convergence near the ghost attractor in a stochastically switching dynamical system to formulate Theorem 2 for approximate synchronization in the stochastic ecological network (2).